Organic Electronics 13 (2012) 673–680

Contents lists available at SciVerse ScienceDirect

Organic Electronics

journal homepage: www.elsevier.com/locate/orgel

Small molecules based on bithiazole for solution-processed organic solar cells

Yuze Lin [a,b], Pei Cheng [a,b], Yao Liu [a,b], Qinqin Shi [a], Wenping Hu [a], Yongfang Li [a], Xiaowei Zhan [a,*]

[a] Beijing National Laboratory for Molecular Sciences and Key Laboratory of Organic Solids, Institute of Chemistry, Chinese Academy of Sciences, Beijing 100190, China
[b] Graduate University of Chinese Academy of Sciences, Beijing 100049, China

ARTICLE INFO

Article history:
Received 20 December 2011
Received in revised form 14 January 2012
Accepted 14 January 2012
Available online 1 February 2012

Keywords:
Bithiazole
Triphenylamine
Conjugated small molecule
Bulk heterojunction
Organic solar cell
Field-effect transistor

ABSTRACT

A series of donor–acceptor–donor small molecules (**1**–**3**) with bithiazole as acceptor unit, triphenylamine as donor unit and thiophene with different number (0, 1, 2) as bridge were synthesized by palladium(0)-catalyzed Suzuki or Stille coupling reactions. The thermal, optical, electrochemical, charge transport, and photovoltaic properties of these small molecules were examined. All compounds exhibit excellent thermal stability with decomposition temperatures (5% weight loss) over 390 °C in nitrogen atmosphere. As increasing the number of thiophene and π-conjugation length of molecule, the absorption maximum in film red shifts from 406 to 498 nm, the extinction coefficient increases from 1.35×10^4 to $7.66 \times 10^4\ M^{-1}\ cm^{-1}$, and the optical band gap decreases from 2.6 to 2.0 eV. The electron-donating thiophene and bithiophene in compounds **2** and **3** up-shift HOMO energy level from −5.42 (**1**) to −5.24 eV (**2**) or −5.22 eV (**3**), and down-shift LUMO energy level from −2.48 (**1**) to −2.84 eV (**2**) or −2.81 eV (**3**). The hole mobility of compound **3** is up to $3.6 \times 10^{-4}\ cm^2\ V^{-1}\ s^{-1}$, which is one order of magnitude higher than that of compound **2**, but compound **1** shows no field-effect transistor performance. Solution-processed bulk heterojunction organic solar cells based on **1**–**3**:$PC_{71}BM$ (1:4, w/w) blend films exhibit increasing power conversion efficiency (up to 2.61%) as increasing thiophene unit number.

1. Introduction

Organic solar cells (OSCs) are a promising cost-effective alternative for utility of solar energy, and possess low-cost, light-weight, and flexibility advantages [1–3]. Much of the focus has been on the development of polymer-based OSCs which have seen a dramatic rise in efficiency over the last decade, and the encouraging power conversion efficiency (PCE) over 8% [4] has been achieved from bulk heterojunction (BHJ) [5] OSCs based on polymer donors and fullerene acceptors. Small molecules offer potential advantages over conjugated polymer counterparts in terms of defined molecular structure, definite molecular weight, high purity, easy purification, easy mass-scale production, and good batch-to-batch reproducibility [6–10]. In recent years, great efforts have been dedicated to develop small molecules for application in OSCs, such as linear donor–acceptor–donor (D–A–D) [11–15] or A-D-A [16–20] molecules, star- or X-shaped molecules [21–28], fused polycyclic arenas [29–32], and other organic dyes [33–42]. So far the highest PCEs of solution-processed BHJ OSCs based on small molecular donors are over 6% [19,42], lower than that (over 8%) of polymeric donors-based BHJ OSCs. Despite the fact that considerable progress has been made in small molecule-based OSCs, the relatively low PCE is hindrance to commercialization of these devices.

Thiazole is a widely used electron-accepting heterocycle due to electron-withdrawing nitrogen of imine (C=N). Small molecules based on bithiazole (BTZ) were used as

* Corresponding author.
E-mail address: xwzhan@iccas.ac.cn (X. Zhan).

1566-1199/$ - see front matter © 2012 Elsevier B.V. All rights reserved.
doi:10.1016/j.orgel.2012.01.016

semiconductors in organic field-effect transistors (OFETs), and exhibited electron mobility as high as 1.83 $cm^2 V^{-1} s^{-1}$ [43]. Conjugated polymers based on BTZ were used as semiconductors in OFETs, and exhibited hole mobility as high as 0.14 $cm^2 V^{-1} s^{-1}$ [44]. Conjugated polymers based on BTZ have been used in OSCs as donors [45–51]. We have systemically explored the design and synthesis of BTZ-containing conjugated polymers and their application in solution-processed OSCs, and PCEs up to 4.46% were achieved in combination with [6,6]-phenyl-C_{71}-butyric acid methyl ester ($PC_{71}BM$) acceptor [52–63]. However, to our knowledge, there has been only one report on BTZ-based small molecules for use in OSCs. Very recently, Lee et al. reported a BTZ-based small molecule for OSCs with a PCE of 1.3% [64].

Triphenylamine (TPA) has been regarded as a promising moiety for organic semiconductor materials owing to its good electron-donating and hole-transporting capability [65]. TPA-based molecules, including star-shaped molecules with TPA as core and linear molecules with D-A-D structure, have been widely investigated for application in OSCs. Recently, our group reported that solution-processed OSCs based on a star-shaped small molecule with TPA as core gave PCEs up to 4.3% without any post-treatments [21], which is the highest reported for solution processed BHJ OSCs based on TPA-based molecules and star-shaped molecules.

Here we report a series of D-A-D molecules with BTZ as acceptor (A) unit, TPA as donor (D) unit and thiophene with different number (0, 1, 2) as bridge (**1**–**3**, Fig. 1). In this system, the molecule with more thiophene units exhibited broader absorption spectra, higher extinction coefficient, and higher hole mobility. Without any post-treatments, solution-processed OSCs based on **3** exhibited promising PCEs as high as 2.61%.

2. Experimental section

2.1. Measurements and characterization

The ^1H and ^{13}C NMR spectra were measured on a Bruker AVANCE 400 MHz spectrometer using tetramethylsilane (TMS; $\delta = 0$ ppm) as an internal standard. Mass spectra were measured on a Bruker Daltonics BIFLEX III MALDI-TOF Analyzer using MALDI mode. Elemental analyses were carried out using a FLASH EA1112 elemental analyzer. Solution (dichloromethane) and thin film (on quartz substrate) UV–vis absorption spectra were recorded on a JΛSCO V-570 spectrophotometer. Electrochemical measurements were carried out under nitrogen on a deoxygenated solution of tetra-*n*-butylammonium hexafluorophosphate (0.1 M) in CH_3CN using a computer-controlled CHI660C electrochemical workstation, a glassy-carbon working electrode coated with sample films, a platinum-wire auxiliary electrode, and an Ag wire anodized with AgCl as a pseudo-reference electrode. Potentials were referenced to ferrocenium/ferrocene ($FeCp_2^{+/0}$) couple by using ferrocene as a standard. Thermogravimetric analysis (TGA) measurements were performed on Shimadzu thermogravimetric analyzer (model DTG-60) under a nitrogen flow at a heating rate of 10 °C min^{-1}. Melting points were measured by micro melting point apparatus RDY-2B at a heating range of 25–250 °C. The nanoscale morphology of blend film was observed by using a Veeco Nanoscopy V atomic force microscopy (AFM) in tapping mode.

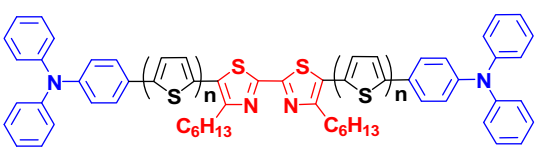

1 n = 0
2 n = 1
3 n = 2

Fig. 1. Chemical structures of compounds **1**–**3**.

2.2. OFET device fabrication and characterization

OFETs based on **1**, **2** or **3** films were fabricated in a bottom gate, top contact configuration at ambient atmosphere. Highly n-doped silicon and thermally grown silicon dioxide (500 nm) were used as back gate and gate dielectric, respectively. The substrates were cleaned sequentially with pure water, hot concentrated sulfuric acid-hydrogen peroxide solution (concentrated sulfuric acid/hydrogen peroxide water = 2:1), pure water, and isopropanol. Then vaporized octadecyltrichlorosilane (OTS) was used for surface modification of the gate dielectric layer. Solutions of **1**, **2** or **3** in chloroform (10 mg mL^{-1}) were spin coated onto OTS treated substrates to form thin films. Gold contacts (25 nm) for source and drain electrodes (finger parallel source-drain geometry) were vacuum-deposited at a rate of 0.1 Å s^{-1} through a metal shadow mask that defined a series of transistor devices with a channel length (L) of 50 μm and a channel width (W) of 1 mm. The characterization was accomplished by keithley 4200 SCS with a micromanipulator 6150 probe station in a clean shielded box at ambient atmosphere. Then field-effect mobility was calculated from the standard equation for saturation region in metal-dioxide-semiconductor field-effect transistors: $I_{DS} = (W/2L)\mu C_i(V_G - V_T)^2$, where I_{DS} is drain-source current, μ is field-effect mobility, W and L are the channel width and length, C_i is the capacitance per unit area of the dielectric layer (C_i = 7.5 nF cm^{-2}), V_G is the gate voltage and V_T is the threshold voltage.

2.3. Fabrication and characterization of photovoltaic cells

OSC devices were fabricated with a structure of ITO/PEDOT:PSS/**1**–**3**:$PC_{71}BM$/Ca/Al. The patterned indium tin oxide (ITO) glass (sheet resistance = 30 Ω $\square^{-1}$) was pre-cleaned in an ultrasonic bath of acetone and isopropanol, and treated in ultraviolet-ozone chamber (Jelight Company, USA) for 30 min. A thin layer (30 nm) of poly(3,4-ethylenedioxythiophene):poly(styrene sulfonate) (PEDOT:PSS, Baytron P VP AI 4083, Germany) was spin-coated onto the ITO glass and baked at 150 °C for 30 min. Ano-dichlorobenzene or chlorobenzene solution of blend of compound **1**, **2**, or **3** with $PC_{71}BM$ was subsequently spin-coated at rotational speed of 2000 rpm on PEDOT:PSS layer to form a photosensitive layer (*ca.* 45 nm). The

thickness of the photosensitive layer was measured by Ambios Technology XP-2 profilometer. Calcium (*ca.* 15 nm) and aluminium (*ca.* 50 nm) layers were subsequently evaporated onto the surface of the photosensitive layer under vacuum (*ca.* 10^{-5} Pa) to form the negative electrode. The active area of the device was 4 mm^2. *J–V* curve was measured with a computer-controlled Keithley 236 Source Measure Unit. A xenon lamp coupled with AM1.5 solar spectra filters was used as the light source, and the optical power at the sample was 100 mW cm^{-2}. The incident photon to converted current efficiency (IPCE) spectra was measured by Stanford Research Systems model SR830 DSP lock-in amplifier coupled with WDG3 monochromator and 500 W xenon lamp.

2.4. Materials

Unless otherwise stated, starting materials were used as commercially purchased without further purification. Toluene was distilled from sodium-benzophenone under nitrogen before use. Reactions were performed under nitrogen atmosphere. 5,5′-Dibromo-4,4′-dihexyl-2,2′-bithiazole [45], 5,5′-bis(5-bromothiophen-2-yl)-4,4′-dihexyl-2, 2′-bithiazole [45], *N*,*N*-diphenyl-4-(tributylstannyl)aniline [66], and *N*,*N*-diphenyl-4-(5-(tributylstannyl) thiophen-2-yl)aniline [66] were synthesized according to the literature procedures.

2.5. Synthesis

2.5.1. 4,4′-(4,4′-dihexyl-2,2′-bithiazole-5,5′-diyl)bis(N,N-diphenylaniline) (**1**)

To a three-necked round bottom flask were added4-(diphenylamino)phenylboronic acid (145 mg, 0.5 mmol), 5,5′-dibromo-4,4′-dihexyl-2,2′-bithiazole (124 mg, 0.25 mmol), toluene (5 mL), potassium carbonate aqueous solution (2 M, 2.5 mL) and tetrabutylammonium bromide (15 mg). The mixture was deoxygenated with nitrogen for 30 min. $Pd(PPh_3)_4$ (50 mg, 0.043 mmol) was added under nitrogen. The mixture was refluxed for 48 h and then cooled down to room temperature. Water (50 mL) was added and the mixture was extracted with dichloromethane (2 × 50 mL). The organic phase was dried over anhydrous $MgSO_4$ and filtered. After removing the solvent from filtrate, the residue was purified by column chromatography on silica gel using petroleum ether/dichloromethane (1:1) as eluent yielding a yellow solid (160 mg, 78%). Melting point (Mp): 146 °C. ^{1}H NMR (400 MHz, CD_2Cl_2): δ 7.26 (m, 12H), 7.11 (d, J = 8.0 Hz, 8H), 7.04 (m, 8H), 2.78 (t, J = 7.6 Hz, 4H), 1.70 (m, 4H), 1.32 (m, 12H), 0.83 (t, J = 5.2 Hz, 6H). ^{13}C NMR (100 MHz, CD_2Cl_2): δ 157.97, 153.46, 147.91, 147.36, 134.00, 130.06, 129.42, 125.02, 124.94, 123.52, 122.68, 31.65, 29.74, 29.12, 22.66, 13.91. MS (MALDI): *m/z* 822 (M^+). Anal. Calcd for $C_{54}H_{54}N_4S_2$: C, 78.79; H, 6.61; N, 6.81. Found: C, 78.77; H, 6.71; N, 6.62%.

2.5.2. 4,4′-(5,5′-(4,4′-dihexyl-2,2′-bithiazole-5,5′-diyl) bis(thiophene-5,2-diyl))bis(N,N-diphenylaniline) (**2**)

To a three-necked round bottom flask were added *N*,*N*-diphenyl-4-(tributylstannyl)aniline (265 mg, 0.5 mmol), 5,5′-bis(5-bromothiophen-2-yl)-4,4′-dihexyl-2,2′-bithiazole (131 mg, 0.2 mmol) and toluene (10 mL). The mixture was deoxygenated with nitrogen for 30 min. $Pd(PPh_3)_4$ (12 mg, 0.01 mmol) was added under nitrogen. The mixture was refluxed for 48 h and then cooled down to room temperature. A solution of KF (1 g) in water (10 mL) was added and stirred at room temperature for 2 h. Water (40 mL) was added and the mixture was extracted with dichloromethane (2 × 50 mL). The organic phase was dried over anhydrous $MgSO_4$ and filtered. After removing the solvent from filtrate, the residue was purified by column chromatography on silica gel using petroleum ether/dichloromethane (10:1) as eluent yielding a red solid (50 mg, 25%). Mp: 160 °C. ^{1}H NMR (400 MHz, $CDCl_3$): δ 7.49 (d, J = 8.1 Hz, 4H), 7.27 (m, 8H), 7.21 (m, 4H), 7.11 (m, 8H), 7.05 (m, 8H), 2.96 (t, J = 6.9 Hz, 4H), 1.79 (m, 4H), 1.48 (m, 4H), 1.32 (m, 8H), 0.87 (m, 6H). ^{13}C NMR (100 MHz, $CDCl_3$): δ 157.42, 154.39, 147.77, 147.55, 145.29, 131.52, 129.50, 128.37, 128.05, 127.70, 126.64, 124.79, 123.53, 123.42, 122.84, 31.82, 30.71, 29.55, 29.38, 22.80, 14.29. MS (MALDI): *m/z* 986 (M^+). Anal. Calcd for $C_{62}H_{58}N_4S_4$: C, 75.42; H, 5.92; N, 5.67. Found: C, 75.14; H, 6.16; N, 5.30%.

2.5.3. 4,4′-(5′,5″-(4,4′-dihexyl-2,2′-bithiazole-5,5′-diyl)bis(2′,2″-bithiophene-5′,5′-diyl))bis(N,N-diphenylaniline) (**3**)

To a three-necked round bottom flask were added *N*,*N*-diphenyl-4-(5-(tributylstannyl)thiophen-2-yl)aniline (308 mg, 0.5 mmol), 5,5′-bis(5-bromothiophen-2-yl)-4,4′-dihexyl-2,2′-bithiazole (130 mg, 0.2 mmol) and toluene (12 mL). The mixture was deoxygenated with nitrogen for 30 min. $Pd(PPh_3)_4$ (40 mg, 0.035 mmol) was added under nitrogen. The mixture was refluxed for 48 h and then cooled down to room temperature. A solution of KF (1 g) in water (12 mL) was added and stirred at room temperature for 2 h. Water (40 mL) was added and the mixture was extracted with dichloromethane (2 × 50 mL). The organic phase was dried over anhydrous $MgSO_4$ and filtered. After removing the solvent from filtrate, the residue was purified by column chromatography on silica gel using petroleum ether/dichloromethane (3:1) as eluent yielding a red solid (170 mg, 75%). Mp: 206 °C. ^{1}H NMR (400 MHz, CD_2Cl_2): δ 7.46 (d, J = 8.5 Hz, 4H), 7.25 (t, J = 7.7 Hz, 8H), 7.17 (m, 6H), 7.13 (d, J = 3.8 Hz, 2H), 7.09 (d, J = 8.0 Hz, 8H), 7.03 (m, 8H), 2.93 (t, J = 7.8 Hz, 4H), 1.50 (m, 4H), 1.33 (m, 12H), 0.87 (t, J = 6.8 Hz, 6H). ^{13}C NMR (100 MHz, CD_2Cl_2): δ 157.50, 154.77, 147.73, 147.49, 143.82, 138.55, 134.96, 131.55, 129.43, 128.32, 127.70, 127.64, 126.42, 125.15, 124.77, 123.94, 123.40, 123.07, 31.75, 30.60, 29.39, 29.26, 22.74, 13.97. MS (MALDI): *m/z* 1150 (M^+). Anal. Calcd for $C_{70}H_{62}N_4S_6$: C, 73.00; H, 5.43; N, 4.86. Found: C, 72.82; H, 5.65; N, 4.50%.

3. Results and discussion

3.1. Synthesis and characterization

The synthetic routes to compounds **1**–**3** are shown in Scheme 1. Compound **1** was synthesized from Suzuki coupling reaction between TPA-boronic acid and BTZ dibromide using $Pd(PPh_3)_4$ as the catalyst. Compounds **2** and **3** were synthesized from Stille coupling reaction between

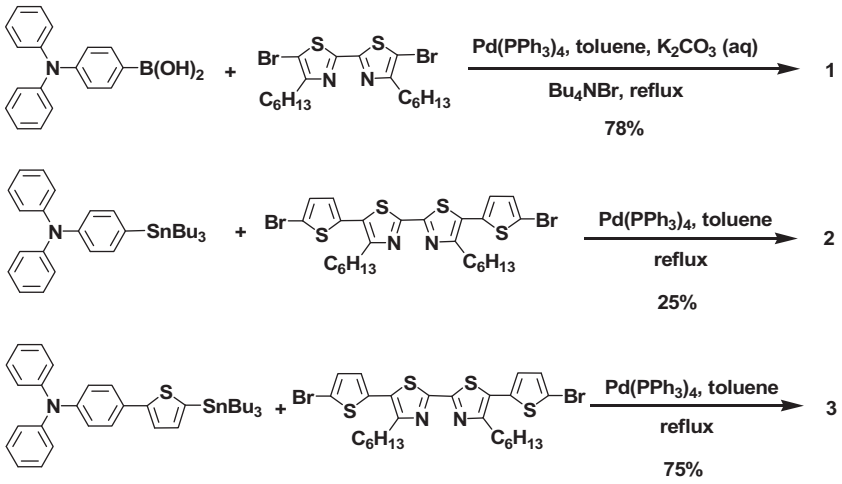

Scheme 1. Synthetic routes to compounds **1**–**3**.

Table 1
Thermal and absorption data and energy levels of compounds **1**–**3**.

	T_d/°C	λ_{max}^{abs}/nm		$E_g^{opt\,a}$/eV	ε^b/M^{-1} cm^{-1}	HOMO/eV	LUMO/eV	E_g^{ecc}/eV
		Solution	Film					
1	405	406	406	2.58	1.35×10^4	−5.42	−2.48	2.94
2	392	450	466	2.21	2.95×10^4	−5.24	−2.84	2.40
3	422	460	498	2.03	7.66×10^4	−5.22	−2.81	2.41

[a] Estimated from the absorption edge in film.
[b] Extinction coefficient at λ_{max} in solution.
[c] Obtained from electrochemistry.

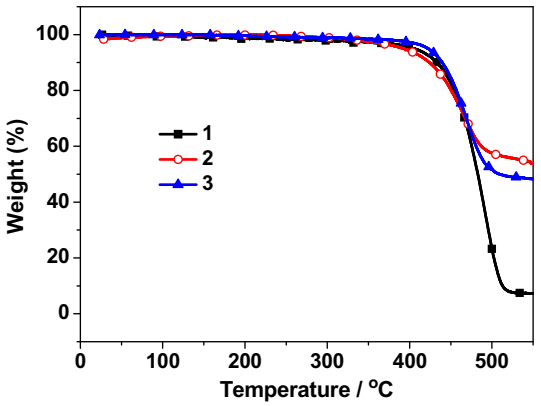

Fig. 2. TGA curves of compounds **1**–**3**.

BTZ-dithiophene dibromide and TPA tin or TPA-thiophene tin, respectively, using $Pd(PPh_3)_4$ as the catalyst. Suzuki coupling reaction using TPA-boronic acid gave a much higher yield than Stille coupling reaction using TPA tin since TPA-boronic acid is easier to purify and has a higher purity than TPA tin. All compounds were fully characterized by MALDI-TOF MS, ^{1}H NMR, ^{13}C NMR, and elemental analysis. Compounds **1**–**3** are readily soluble in common organic solvents such as dichloromethane, dichlorobenzene and chloroform at room temperature, due to two solubilizing *n*-hexyl substituents.

The thermal properties of **1**–**3** were investigated by thermogravimetric analysis (TGA). All compounds have excellent thermal stability with decomposition temperatures (T_d, 5% weight loss) over 390 °C in nitrogen atmosphere (Table 1, Fig. 2). Compounds **1**–**3** are crystalline with a melting point of 146, 160 and 206 °C, respectively.

3.2. Optical properties

The normalized spectra of optical absorption of compounds **1**–**3** in dichloromethane solution (10^{-6} M) and in solid films are shown in Fig. 3. Compounds **1**–**3** in solution exhibit absorption maxima at 406–460 nm with extinction coefficients of 1.3–7.7 × 10^4 M^{-1} cm^{-1} (Table 1). As increasing the number of thiophene unit and the π-conjugated length of molecule, the absorption spectra in film red shift ca. 90 nm, the extinction coefficients increase from 1.35×10^4 to 7.66×10^4 M^{-1} cm^{-1}, and the optical band gaps (E_g^{opt}) estimated from the absorption edge of the thin film decrease from 2.58 to 2.03 eV. In particular, thin films of **3** show significant absorption throughout the visible, which red shifts 38 nm relative to that in solution, indicating that self-organization behavior somewhat exists in the film. However, the film of **1** exhibits almost same absorption as

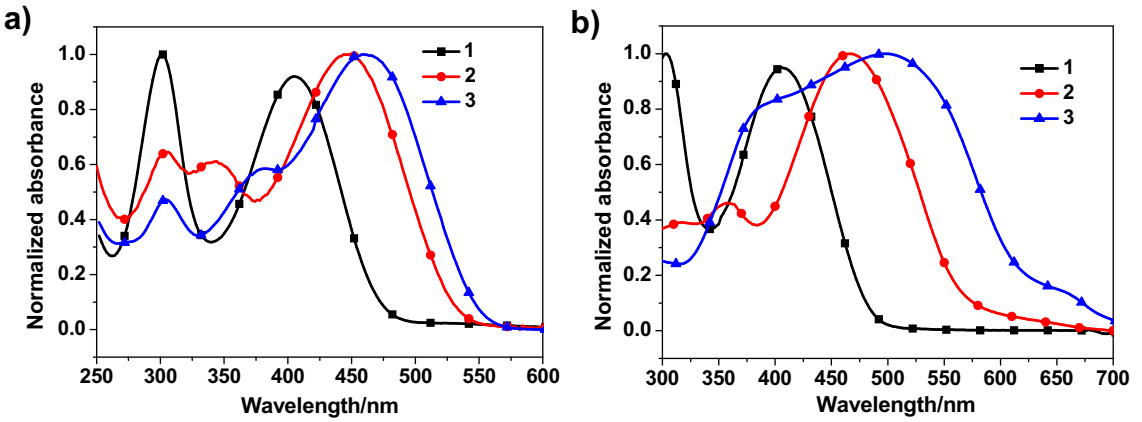

Fig. 3. UV–vis absorption spectra of **1**–**3** in dichloromethane solution (a) and in thin film (b).

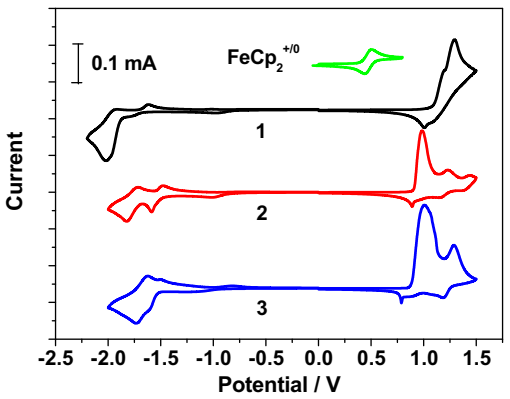

Fig. 4. Cyclic voltammograms for **1**–**3** in CH_3CN/0.1 M $[^nBu_4N]^+[PF_6]^-$ at 100 mV s^{-1}. The horizontal scale refers to an anodized Ag wire pseudo-reference electrode.

that in solution. This result indicates that the increase in thiophene unit could improve the intermolecular interaction in the film and generate strong tendency to absorb the low-energy photons.

3.3. Electrochemical properties

To determine the highest occupied molecular orbital (HOMO) and lowest unoccupied molecular orbital (LUMO) positions of **1**–**3**, cyclic voltammetry (CV) was carried out on these compounds using films on glassy carbon working electrode in 0.1 M $[^nBu_4N]^+[PF_6]^-$ CH_3CN solution at a potential scan rate of 100 mV s^{-1} (Fig. 4). The HOMO and LUMO values of compounds **1**–**3** are estimated from the onset oxidation and reduction potentials, assuming the absolute energy level of $FeCp_2^{+/0}$ to be 4.8 eV below vacuum (oxidation potential of $FeCp_2^{+/0}$ versus Ag wire was measured to be 0.47 V). The electron-donating thiophene and bithiophene π-bridges in compounds **2** and **3** up-shift HOMO energy level from −5.42 eV for compound **1** to −5.24 eV for **2** or −5.22 eV for **3**, and down-shift LUMO energy level from −2.48 eV for compound **1** to −2.84 eV for **2** or −2.81 eV for **3** due to extended π-conjugation and electron delocalization (Table 1). The HOMO-LUMO gaps (E_g^{ec}) obtained from electrochemistry are 2.94 to 2.40 eV, 0.19 to 0.38 eV larger than the optical band gaps (2.58 to 2.03 eV). This phenomenon was also observed for some bithiazole-based polymers in literatures [52,58,67].

3.4. Organic field-effect transistors

The high hole mobility (μ_h) is a basic requirement for effective photovoltaic active donors, to ensure effective charge carrier transport to the electrodes and reduce the photocurrent loss in OSCs. To measure hole mobility of these compounds, OFETs based on **1**–**3** were fabricated on octadecyltrichlorosilane-treated SiO_2/Si substrates through spin-coating process. In a top contact geometry using Au as the source and drain electrodes, compounds **2** and **3** both exhibit typical p-type semiconductor behavior in air, but compound **1** shows no OFET performance, which may be ascribed to its short π-conjugated length (Fig. 5). Due to the relatively long π-conjugated length, the hole mobility in the saturation regime of compound **3** is up to 3.6×10^{-4} cm^2 V^{-1} s^{-1}, which is comparable to those of BTZ-based polymers [59], and one order of magnitude higher than that of compound **2** (Table 2). Thus, the increase in thiophene unit in **1**–**3** extends π-conjugation, improve intermolecular interaction in the film, and finally promotes charge transport. Since OFET mobility measurement is in a different direction to OSCs these results should be interpreted with caution.

3.5. Photovoltaic properties

We investigated the potential of compounds **1**–**3** for OSCs. The compounds were used as donor blending with $PC_{71}BM$ acceptor to fabricate BHJ OSCs with a device structure of ITO/PEDOT:PSS/**1**–**3**:$PC_{71}BM$/Ca/Al. We examined different weight ratios (2:1, 1:1, 1:2, 1:3, and 1:4) of donor:acceptor and found that the weight ratio of 1:4 gave the best blend film quality. So we chose the weight ratio of 1:4 for further device investigation. At donor:acceptor weight ratio of 1:4 using chlorobenzene (CB) as spin

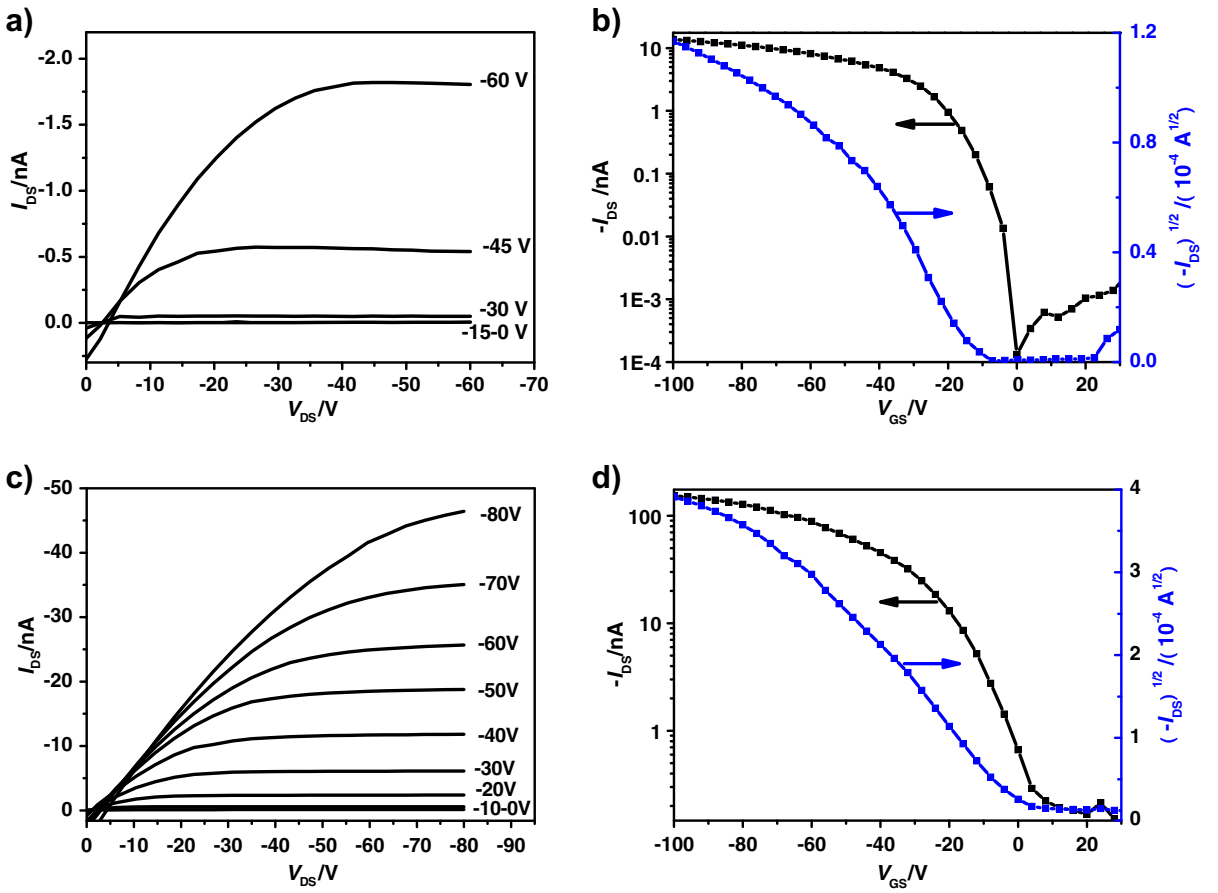

Fig. 5. Typical current-voltage characteristics (I_{DS} vs. V_{DS}) at different gate voltages (V_{GS}), and $-I_{DS}$ and $(-I_{DS})^{1/2}$ vs V_{GS} plots at V_{DS} of −100 V for a top contact device based on **2** (a, b) and **3** (c, d).

Table 2
Performance of OFETs and OSCs based on **1**–**3**.

Compound	OFETs	**1**–**3**: $PC_{71}BM$ (w/w)	Solvent	OSCs			
	μ_h/cm^2 V^{-1} s^{-1}			V_{OC}/V	J_{SC}/mA cm^{-2}	FF	PCE (%)
1	–	1:4	CB	0.71	3.42	0.301	0.73
2	6.5×10^{-5}	1:4	CB	0.81	4.69	0.335	1.27
3	3.6×10^{-4}	1:4	CB	0.79	5.63	0.365	1.63
3		1:4	DCB	0.84	7.72	0.402	2.61

coating solvent, OSCs based on **1**–**3** exhibited increasing short-circuit current density (J_{SC}), fill factor (FF), and PCE benefiting from the broader and stronger absorption as well as higher hole mobility as increasing thiophene unit number of the π-bridge in the molecules (Fig. 6, Table 2). The HOMO level of **1** was the lowest, so the open-circuit voltage (V_{oc}) of **1**-based OSCs was supposed to be the highest. However, the V_{oc} is the smallest. In addition to the difference between the LUMO of $PC_{71}BM$ and the HOMO of donor, mobility and morphology of the active layer also need to be taken into account for V_{oc} [68–70]. For **1**, the lowest V_{oc} is most likely attributed to charge recombination losses at the donor/fullerene interfaces and at the electrodes due to low mobility. Using o-dichlorobenzene (DCB) as spin coating solvent, **3**-based devices exhibited better performance: V_{OC} of 0.84 V, J_{SC} of 7.72 mA cm^{-2}, FF of 0.402, and PCE of 2.61%. As increasing thiophene number, the blend of **1**–**3**:$PC_{71}BM$ (1:4, w/w) exhibited higher incident photon to converted current efficiency (IPCE) (Fig. 7), which is consistent with the tendency of the J_{SC} in OSCs. Replacing CB with DCB as spin coating solvent led to even higher IPCE.

The active layer morphology of OSC devices was examined by atomic force microscope (AFM) technique in tapping mode. Fig. 8 shows the AFM height and phase images of the blend films of **1**–**3**:$PC_{71}BM$ (1:4, w/w)

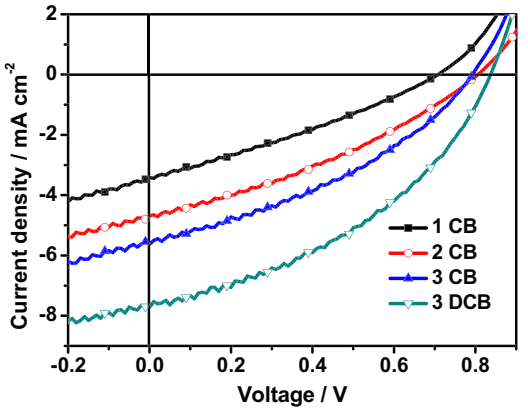

Fig. 6. *J–V* curves of devices with the structure ITO/PEDOT:PSS/**1**–**3**:$PC_{71}BM$(1:4, w/w)/Ca/Al under the illumination of an AM1.5 solar simulator, 100 mW cm^{-2}.

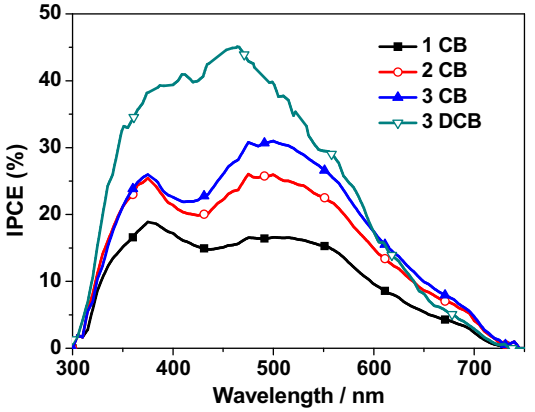

Fig. 7. IPCE spectra of devices with the structure ITO/PEDOT:PSS/**1**–**3**:$PC_{71}BM$(1:4, w/w)/Ca/Al.

without any post-treatments. The blend films based **1**–**3** exhibited typical cluster structures with many aggregated domains and root-mean-square (RMS) roughness of 0.32–0.45 nm. The domain sizes estimated by cross-section profiles are about tens of nanometers. Replacing CB with DCB as spin coating solvent led to reduced phase separation size. These nanoscale aggregated domains are beneficial for charge separation and enhanced efficiency of the OSCs.

4. Conclusions

We have designed and synthesized D-A-D small molecules **1**–**3** with BTZ as acceptor unit, TPA as donor unit and thiophene with different number (0, 1, 2) as π-bridges. **1**–**3** showed excellent thermal stability and solubility in common organic solvents. As increasing the number of thiophene unit of the π-bridges and the π-conjugation length of molecule, the absorption spectrum red shifted, the extinction coefficient increased, and the optical band gap decreased. The electron-donating thiophene and bithiophene π-bridges in compounds **2** and **3** up-shifted HOMO energy level and down-shifted LUMO energy level due to extended π-conjugation and electron delocalization. The increase in thiophene unit in **1**–**3** extended π-conjugation, improved intermolecular interaction in the film, and finally promoted charge transport. BHJ OSCs based on **1**–**3**:$PC_{71}BM$ (1:4, w/w) blend films exhibited increasing J_{SC}, FF, and PCE benefiting from broader and stronger absorption as well as higher hole mobility as increasing thiophene unit number of the π-bridges in the molecules. Using dichlorobenzene as spin coating solvent, **3**-based devices exhibited best performance: V_{OC} of 0.84 V, J_{SC} of 7.72 mA cm^{-2}, FF of 0.402, and PCE of 2.61%. This result demonstrates that BTZ-based small molecules are promising donor materials for solution processed BHJ OSCs.

Acknowledgements

We thank the NSFC (21025418, 51011130028, 21021091), the 973 Project (2011CB808401), and the Chinese Academy of Sciences for financial support.

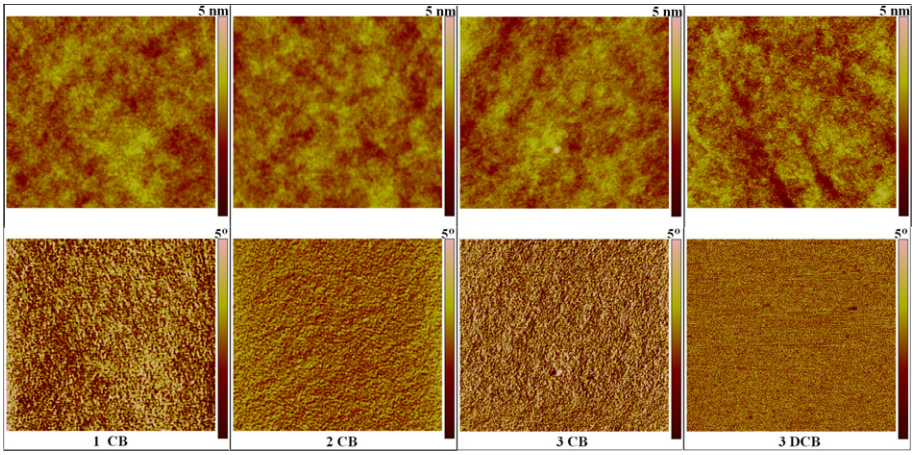

Fig. 8. AFM topography (top) and phase (bottom) images of **1**–**3**:$PC_{71}BM$ (1:4, w/w, CB) and **3**:$PC_{71}BM$ (1:4, w/w, DCB) blend films (3 × 3 μm).

References

[1] X. Zhan, D. Zhu, Polym. Chem. 1 (2010) 409.
[2] Y.-J. Cheng, S.-H. Yang, C.-S. Hsu, Chem. Rev. 109 (2009) 5868.
[3] J. Chen, Y. Cao, Acc. Chem. Res. 42 (2009) 1709.
[4] Z. He, C. Zhong, X. Huang, W.-Y. Wong, H. Wu, L. Chen, S. Su, Y. Cao, Adv. Mater. 23 (2011) 4636.
[5] G. Yu, J. Gao, J.C. Hummelen, F. Wudl, A.J. Heeger, Science 270 (1995) 1789.
[6] B. Walker, C. Kim, T.-Q. Nguyen, Chem. Mater. 23 (2011) 470.
[7] M. Lloyd, J. Anthony, G. Malliaras, Mater. Today 10 (2007) 34.
[8] A.W. Hains, Z. Liang, M.A. Woodhouse, B.A. Gregg, Chem. Rev. 110 (2010) 6689.
[9] J. Roncali, Acc. Chem. Res. 42 (2009) 1719.
[10] Y. Li, Q. Guo, Z. Li, J. Pei, W. Tian, Energy Environ. Sci. 3 (2010) 1427.
[11] H. Shang, H. Fan, Q. Shi, S. Li, Y. Li, X. Zhan, Sol. Energy Mater. Sol. Cells 94 (2010) 457.
[12] H. Fan, H. Shang, Y. Li, X. Zhan, Appl. Phys. Lett. 97 (2010) 133302.
[13] Q. Shi, P. Cheng, Y. Li, X. Zhan, Adv. Energy Mater. 2 (2012) 63.
[14] B. Walker, A.B. Tamayo, X.-D. Dang, P. Zalar, J.H. Seo, A. Garcia, M. Tantiwiwat, T.-Q. Nguyen, Adv. Funct. Mater. 19 (2009) 3063.
[15] X. Zhao, C. Piliego, B. Kim, D.A. Poulsen, B. Ma, D.A. Unruh, J.M.J. Fréchet, Chem. Mater. 22 (2010) 2325.
[16] S. Loser, C.J. Bruns, H. Miyauchi, R.o.P. Ortiz, A. Facchetti, S.I. Stupp, T.J. Marks, J. Am. Chem. Soc. 133 (2011) 8142.
[17] Y. Liu, X. Wan, F. Wang, J. Zhou, G. Long, J. Tian, J. You, Y. Yang, Y. Chen, Adv. Energy Mater. 1 (2011) 771.
[18] Y. Liu, X. Wan, F. Wang, J. Zhou, G. Long, J. Tian, Y. Chen, Adv. Mater. 23 (2011) 5387.
[19] Z. Li, G. He, X. Wan, Y. Liu, J. Zhou, G. Long, Y. Zuo, M. Zhang, Y. Chen, Adv. Energy Mater. 2 (2012) 74.
[20] J. Zhou, X. Wan, Y. Liu, G. Long, F. Wang, Z. Li, Y. Zuo, C. Li, Y. Chen, Chem. Mater. 23 (2011) 4666.
[21] H. Shang, H. Fan, Y. Liu, W. Hu, Y. Li, X. Zhan, Adv. Mater. 23 (2011) 1554.
[22] H. Shang, H. Fan, Y. Liu, W. Hu, Y. Li, X. Zhan, J. Mater. Chem. 21 (2011) 9667.
[23] J. Zhang, D. Deng, C. He, Y. He, M. Zhang, Z.-G. Zhang, Z. Zhang, Y. Li, Chem. Mater. 23 (2011) 817.
[24] J. Zhang, Y. Yang, C. He, Y. He, G. Zhao, Y. Li, Macromolecules 42 (2009) 7619.
[25] W. Li, C. Du, F. Li, Y. Zhou, M. Fahlman, Z. Bo, F. Zhang, Chem. Mater. 21 (2009) 5327.
[26] E. Ripaud, T. Rousseau, P. Leriche, J. Roncali, Adv. Energy Mater. 1 (2011) 540.
[27] S. Roquet, R. de Bettignies, P. Leriche, A. Cravino, J. Roncali, J. Mater. Chem. 16 (2006) 3040.
[28] S. Roquet, A. Cravino, P. Leriche, O. Aleveque, P. Frere, J. Roncali, J. Am. Chem. Soc. 128 (2006) 3459.
[29] K.N. Winzenberg, P. Kemppinen, G. Fanchini, M. Bown, G.E. Collis, C.M. Forsyth, K. Hegedus, T.B. Singh, S.E. Watkins, Chem. Mater. 21 (2009) 5701.
[30] W.W.H. Wong, C.-Q. Ma, W. Pisula, C. Yan, X. Feng, D.J. Jones, K. Mullen, R.A.J. Janssen, P. Bauerle, A.B. Holmes, Chem. Mater. 22 (2010) 457.
[31] M.T. Lloyd, A.C. Mayer, S. Subramanian, D.A. Mourey, D.J. Herman, A.V. Bapat, J.E. Anthony, G.G. Malliaras, J. Am. Chem. Soc. 129 (2007) 9144.
[32] P. Dutta, W. Yang, S.H. Eom, W.-H. Lee, I.N. Kang, S.-H. Lee, Chem. Commun. 48 (2012) 573.
[33] F. Silvestri, M.D. Irwin, L. Beverina, A. Facchetti, G.A. Pagani, T.J. Marks, J. Am. Chem. Soc. 130 (2008) 17640.
[34] D. Bagnis, L. Beverina, H. Huang, F. Silvestri, Y. Yao, H. Yan, G.A. Pagani, T.J. Marks, A. Facchetti, J. Am. Chem. Soc. 132 (2010) 4074.
[35] N.M. Kronenberg, V. Steinmann, H. Bürckstümmer, J. Hwang, D. Hertel, F. Würthner, K. Meerholz, Adv. Mater. 22 (2010) 4193.
[36] U. Mayerhöffer, K. Deing, K. Gruß, H. Braunschweig, K. Meerholz, F. Würthner, Angew. Chem. Int. Ed. 48 (2009) 8776.
[37] N.M. Kronenberg, M. Deppisch, F. Wurthner, H.W.A. Lademann, K. Deing, K. Meerholz, Chem. Commun. (2008) 6489.
[38] H. Bürckstümmer, E.V. Tulyakova, M. Deppisch, M.R. Lenze, N.M. Kronenberg, M. Gsänger, M. Stolte, K. Meerholz, F. Würthner, Angew. Chem. Int. Ed. 50 (2011) 11628.
[39] T. Rousseau, A. Cravino, T. Bura, G. Ulrich, R. Ziessel, J. Roncali, Chem. Commun. (2009) 1673.
[40] T. Rousseau, A. Cravino, E. Ripaud, P. Leriche, S. Rihn, A. De Nicola, R. Ziessel, J. Roncali, Chem. Commun. 46 (2010) 5082.
[41] P.F. Xia, X.J. Feng, J. Lu, S.-W. Tsang, R. Movileanu, Y. Tao, M.S. Wong, Adv. Mater. 20 (2008) 4810.
[42] Y. Sun, G.C. Welch, W.L. Leong, C.J. Takacs, G.C. Bazan, A.J. Heeger, Nat. Mater. 11 (2012) 44.
[43] S. Ando, R. Murakami, J.-i. Nishida, H. Tada, Y. Inoue, S. Tokito, Y. Yamashita, J. Am. Chem. Soc. 127 (2005) 14996.
[44] J. Liu, R. Zhang, I. Osaka, S. Mishra, A.E. Javier, D.-M. Smilgies, T. Kowalewski, R.D. McCullough, Adv. Funct. Mater. 19 (2009) 3427.
[45] J. Lee, B.-J. Jung, S.K. Lee, J.-I. Lee, H.-J. Cho, H.-K. Shim, J. Polym. Sci., Part A: Polym. Chem. 43 (2005) 1845.
[46] J.-H. Huang, K.-C. Li, D. Kekuda, H.H. Padhy, H.-C. Lin, K.-C. Ho, C.-W. Chu, J. Mater. Chem. 20 (2010) 3295.
[47] W.-Y. Wong, X.-Z. Wang, Z. He, K.-K. Chan, A.B. Djurišić, K.-Y. Cheung, C.-T. Yip, A.M.-C. Ng, Y.Y. Xi, C.S.K. Mak, W.-K. Chan, J. Am. Chem. Soc. 129 (2007) 14372.
[48] K.-C. Li, J.-H. Huang, Y.-C. Hsu, P.-J. Huang, C.-W. Chu, J.-T. Lin, K.-C. Ho, K.-H. Wei, H.-C. Lin, Macromolecules 42 (2009) 3681.
[49] J.-H. Huang, K.-C. Li, F.-C. Chien, Y.-S. Hsiao, D. Kekuda, P. Chen, H.-C. Lin, K.-C. Ho, C.-W. Chu, J. Phys. Chem. C 114 (2010) 9062.
[50] I.H. Jung, J. Yu, E. Jeong, J. Kim, S. Kwon, H. Kong, K. Lee, H.Y. Woo, H.K. Shim, Chem.-Eur. J. 16 (2010) 3743.
[51] D. Patra, D. Sahu, H. Padhy, D. Kekuda, C.W. Chu, H.C. Lin, J. Polym. Sci., Part A: Polym. Chem. 48 (2010) 5479.
[52] M. Zhang, X. Guo, X. Wang, H. Wang, Y. Li, Chem. Mater. 23 (2011) 4264.
[53] M. Zhang, H. Fan, X. Guo, Y. He, Z.-G. Zhang, J. Min, J. Zhang, G. Zhao, X. Zhan, Y. Li, Macromolecules 43 (2010) 8714.
[54] M. Zhang, H. Fan, X. Guo, Y. He, Z. Zhang, J. Min, J. Zhang, G. Zhao, X. Zhan, Y. Li, Macromolecules 43 (2010) 5706.
[55] M. Zhang, Y. Sun, X. Guo, C. Cui, Y. He, Y. Li, Macromolecules 44 (2011) 7625.
[56] M. Zhang, X. Guo, Y. Li, Macromolecules 44 (2011) 8798.
[57] H. Wang, Q. Shi, Y. Lin, H. Fan, P. Cheng, X. Zhan, Y. Li, D. Zhu, Macromolecules 44 (2011) 4213.
[58] Q. Shi, H. Fan, Y. Liu, J. Chen, L. Ma, W. Hu, Z. Shuai, Y. Li, X. Zhan, Macromolecules 44 (2011) 4230.
[59] Q. Shi, H. Fan, Y. Liu, W. Hu, Y. Li, X. Zhan, J. Phys. Chem. C 114 (2010) 16843.
[60] M. Yang, B. Peng, B. Liu, Y. Zou, K. Zhou, Y. He, C. Pan, Y. Li, J. Phys. Chem. C 114 (2010) 17989.
[61] M. Zhang, H. Fan, X. Guo, Y. Yang, S. Wang, Z.-G. Zhang, J. Zhang, X. Zhan, Y. Li, J. Polym. Sci., Part A: Polym. Chem. 49 (2011) 2746.
[62] Q. Shi, H. Fan, Y. Liu, J. Chen, Z. Shuai, W. Hu, Y. Li, X. Zhan, J. Polym. Sci., Part A: Polym. Chem. 49 (2011) 4875.
[63] H. Fan, M. Zhang, X. Guo, Y. Li, X. Zhan, ACS Appl. Mater. Interfaces 3 (2011) 3646.
[64] P. Dutta, W. Yang, S.H. Eom, S.-H. Lee, Org. Electron. 13 (2012) 273.
[65] Z. Ning, H. Tian, Chem. Commun. (2009) 5483.
[66] J. Liu, X. Guo, L.J. Bu, Z.Y. Xie, Y.X. Cheng, Y.H. Geng, L.X. Wang, X.B. Jing, F.S. Wang, Adv. Funct. Mater. 17 (2007) 1917.
[67] H. Kong, S. Cho, D.H. Lee, N.S. Cho, M.-J. Park, I.H. Jung, J.-H. Park, C.E. Park, H.-K. Shim, J. Polym. Sci., Part A: Polym. Chem. 49 (2011) 2886.
[68] Z. Li, J. Ding, N. Song, X. Du, J. Zhou, J. Lu, Y. Tao, Chem. Mater. 23 (2011) 1977.
[69] M.C. Scharber, D. Wuhlbacher, M. Koppe, P. Denk, C. Waldauf, A.J. Heeger, C.L. Brabec, Adv. Mater. 18 (2006) 789.
[70] S.Q. Xiao, A.C. Stuart, S.B. Liu, H.X. Zhou, W. You, Adv. Funct. Mater. 20 (2010) 635.